MATHEMATICAL MODELING OF SECTIONS OF VARIABLE RIGIDITY IN FRONT OF ARTIFICIAL STRUCTURES

Vinogradov, Valentin V., *Russian University of Transport, Moscow, Russia.*
Loktev, Alexey A., *Russian University of Transport, Moscow, Russia.*
Fazilova, Zulfiya T., *Russian University of Transport, Moscow, Russia.*

ABSTRACT

The article deals with the features of the transition zone from the ballast under-sleeper base to the bridge structure with various types of span structures, as well as the sections of the ballastless track, conjugated with the transient zone. An analytical model is proposed for describing the dynamic behavior of a railway track in the form of a transversely isotropic plate with variable rigidity parameters. Examples of the use of the proposed model for calculating the dynamic depression of a roadbed under the influence of a rolling stock with different freight and speed characteristics are given.

Keywords: *railway, bridge, roadbed, residual deformation, variable rigidity section, track depression, slope, elastic wave, track profile, transversal-isotropic plate.*

Background. *When reconstructing railway sections for organization of high-speed train traffic, all problem areas that can become sources of large track disturbances and possible speed limits restrictions must be upgraded.*

One of these objects is the railway track on the roadbed in the zone adjacent to the bridge. The track on the bridge itself is quite stable and does not have large drawdowns, while track on the roadbed might be subject to depression in the approach zone. In order to reduce the potential danger, it is necessary to strengthen the track in this zone. To smoothly interface problem areas at the approaches and on the bridges with ballast and ballastless design of the roadbed, transitional sections with variable rigidity are arranged so that the vertical rigidity on the bridge and the approach embankment does not differ much from each other.

Objective. *The objective of the authors is to consider mathematical modeling of sections of variable rigidity in front of artificial structures.*

Methods. *The authors use general scientific and engineering methods, comparative analysis, graph construction, evaluation approach, mathematical calculations.*

Results.

1.

The length of the transition section of the railway track with variable rigidity at the approach to the bridge is determined for each object by the length of the railway track disturbance zone. The data of the track measuring car or the results of the load train tests help in this.

Table 1 shows the minimum length of the section with variable rigidity at the approach to the bridge, depending on the train speed [1].

In studies conducted by Holland Railconsult [2], the length of the transition zone effect can be determined using the so-called «one second» rule. In this case, for example, at a train speed of 200 km/h, the length of the zone will be 55 m.

Table 1

Minimum length of a section of variable rigidity

No.	Minimum length of a section, m	Maximum speed of train movement, km/h
1	15	less than 80
2	20	80–120
3	25	more than 120

When the rolling stock passes through the part of the bend that has arisen during the track depression, an additional dynamic effect on the wheel set occurs, the value of which depends on the size of the difference (angle) in the transition zone (Pic. 1). Increased vibrodynamic load leads to increased wear of the elements of the track upper structure and the appearance of defects in the upper layers of the roadbed.

The intensity of the effect of the vibrodynamic load on the rolling stock can be calculated from the formula:

$$\rho_0 = \frac{1,3\,P_n}{l_{rb} b_0}, \qquad (1)$$

where P is axial load of the calculated mobile unit, kN;

n – number of axles in the bogie;

l_{rb} – length of the rigid base of the bogie, m;

b_0 – length of sleepers, m (for reinforced concrete sleepers – 2,7 m, for wooden sleepers – 2,75 m).

There are many methods and computational algorithms to solve the problems of calculating the structures, their elements and entire structures for different types of applied load, but the most relevant are the techniques that allow to take into account not only the dynamics of the application of the load, but also the dynamics of the changes in deformation and strength characteristics of the structures of track and base [3].

Having the data of field observations, it is possible to construct a mathematical model of a section of variable rigidity using numerical methods in a software environment with the help of a computer and obtain a package of functional requirements and standards for transient structures.

In most modern computer systems (PC Lira, Mirage, SCAD, Ansys, Abaqus, Nastran, Lusas, etc.), the advantage is given to the methods of finite and boundary elements [4–6].

The finite element method replaces the problem of finding a function for the problem of finding the final number of its most accurate values at different nodal points. The primary problem with respect to a function is constructed from a functional equation, the problem of the finite element method with respect to its values at nodes implies a violation of the system of algebraic equations. While reducing the maximum size of the constituent elements, the number of nodes and the required nodal parameters are added. At the same time, the chance to approach the conditions of the problem more accurately and to approach the desired result closely increases.

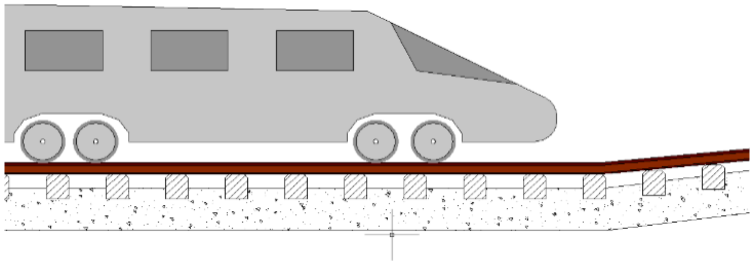

Pic. 1. The section of conjugation of structures of different rigidity.

2.

In our version, it is proposed to represent a railway track as an elastic orthotropic plate [3, 4, 7] whose dynamic behavior is described by equations of the Ufland–Mindlin–Reissner type, taking into account the inertia of rotation of the cross sections and the deformation of the transverse shear [8, 9]. Since the motion of a vehicle in a straight section is actually an axisymmetric problem, then the equations, describing it, can be represented in a general form when the wave characteristics do not depend on the angle θ [10]:

$$D_r\left(\frac{\partial^2\varphi}{\partial r^2}+\frac{1}{r}\frac{\partial\varphi}{\partial r}\right)-D_\theta\frac{\varphi}{r^2}+hKG_{rz}\left(\frac{\partial w}{\partial r}-\varphi\right)=-\rho\frac{h^3}{12}\frac{\partial^2\varphi}{\partial t^2},$$

(2)

$$KG_{rz}\left(\frac{\partial^2 w}{\partial r^2}-\frac{\partial\varphi}{\partial r}\right)+KG_{rz}\frac{1}{r}\left(\frac{\partial w}{\partial r}-\varphi\right)=\rho\frac{\partial^2 w}{\partial t^2}, \qquad (3)$$

$$C_r\left(\frac{\partial^2 u}{\partial r^2}+\frac{1}{r}\frac{\partial u}{\partial r}\right)-C_\theta\frac{u}{r^2}=\rho h\frac{\partial^2 u}{\partial t^2}, \qquad (4)$$

$$C_k\left(\frac{\partial^2 v}{\partial r^2}+\frac{1}{r}\frac{\partial v}{\partial r}-\frac{v}{r^2}\right)=\rho h\frac{\partial^2 v}{\partial t^2}, \qquad (5)$$

$$D_k\left(\frac{\partial^2\psi}{\partial r^2}+\frac{1}{r}\frac{\partial\psi}{\partial r}-\frac{\psi}{r^2}\right)-KhG_{\theta z}\psi=-\rho\frac{h^3}{12}\frac{\partial^2\psi}{\partial t^2}, \qquad (6)$$

where

$$D_r=\frac{h^3}{12}B_r,\quad D_\theta=\frac{h^3}{12}B_\theta,\quad D_k=\frac{h^3}{12}B_k,$$

$$C_r=hB_r,\quad C_\theta=hB_\theta,\quad C_k=hB_k,$$

$$D_{r\theta}=D_r\sigma_\theta+2D_k,$$

$$B_r=\frac{E_r}{1-\sigma_r\sigma_\theta},\ B_\theta=\frac{E_\theta}{1-\sigma_r\sigma_\theta},\ B_k=G_{r\theta},$$

$E_r\sigma_r=E_\theta\sigma_\theta,\ K=\frac{5}{6};$ *D_r, D_θ and C_r, C_θ – respectively, rigidity of deflection and tension-compression for directions r, θ; D_k – torsional rigidity; C_k – shear rigidity; E_r, E_θ and σ_r, σ_θ – elastic modulus and Poisson's ratio for directions r, θ; G_{rz}, $G_{\theta z}$ – shear modulus in the planes rz and θz respectively; w(r, θ) – normal displacement of the median plane; u(r, θ) and v(r, θ) – tangential displacements of the median surface, respectively, with respect to the coordinates r, θ; φ(r, θ) and ψ(r, θ) – arbitrary sought functions of the coordinates r, θ.*

If we consider the deformation of the ballastless track, then the proposed model can be simplified by assuming that the base plate can be represented by a transversally isotropic plate lying on the deformable base, two edges of which are rigidly fixed (along the track, in the direction of the rails), and the other two

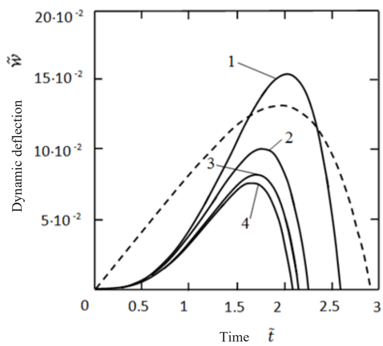

Pic. 3. Dependence of the dynamic deflection on time for different values of the ratio E_θ/E_r.

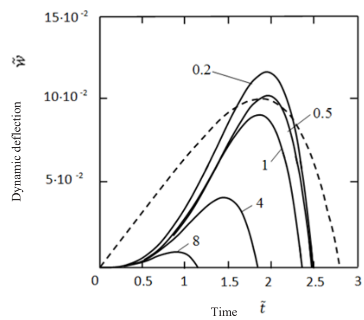

Pic. 4. Dependence of the dynamic deflection on time for different values of the ratio G_{rz}/E_r.

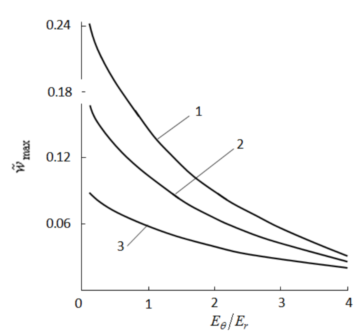

Pic. 5. Dependence of the maximum deflection on the relation E_θ/E_r for different values of $\tilde{E}$.

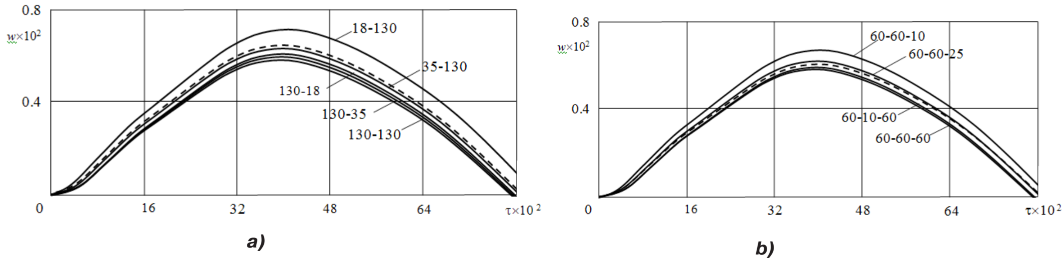

Pic. 6. Dependence of the dynamic deflection at the point of impact on time for different values in the anisotropy directions: a) moduli of deformation, b) shear moduli.

are hinged (across the track, in the direction of sleepers) [11–13]. In this case, the plate in the non-deformable state occupies the area $\{0 \le x \le l_1; 0 \le y \le l_2; -h \le z \le h\}$.

To complete the simulation of dynamic behavior and calculation of the first and second group of limiting states of a reinforced concrete slab, the initial problem is to be presented as a set of simpler ones, and the first problem in this series is to determine the natural vibrations of the plate. The equation describing the proper transverse vibrations of the plate can be obtained from the relations (2) –(6) and written in the form [15]:

$$A_1 \frac{\partial^2 W}{\partial t^2} + A_2 \frac{\partial^4 W}{\partial t^4} - A_3 \frac{\partial^2}{\partial t^2} \Delta W + \\ + A_4 \Delta^2 W + P(W) = 0, \qquad (7)$$

where W – transverse displacement of the points of the medium plane of the plate, Δ *– Laplace operator.*

$$A_1 = \rho_1; A_2 = \rho_1^2 \left(A_{33}^{-1} + 3A_{44}^{-1}\right)\frac{h^2}{b};$$
$$A_3 = \left\{-\rho_1 \left[\begin{matrix} 2 - 2A_{11}A_{33}^{-1} - \\ -3\left(A_{13}^2 - A_{11}A_{33}\right)A_{33}^{-1}A_{44}^{-1} \end{matrix}\right]\right\}\frac{h^2}{b};$$
$$A_4 = 2A_{33}^{-1}\left(A_{11}A_{33} - A_{13}^2\right)\frac{h^2}{b}; A_5 = \frac{S}{2h}\rho_1;$$
$$A_6 = \frac{S}{2h}\rho_1 \frac{h^2}{2}\left(\rho_1 A_{44}^{-1} + 3A_{33}^{-1}\right); A_7 = \\ = -4\frac{S}{2h}\rho_1 A_{11} A_{33}^{-1}. \qquad (8)$$

In those ratios, the value

$$P(W) = A_5 \frac{\partial W}{\partial t} + A_6 \frac{\partial^3 W}{\partial t^3} + A_7 \Delta \frac{\partial W}{\partial t} \text{ —}$$

determines the reaction of the base, ρ_1 *is density, b – speed of the transverse wave;* $A_{11} = A_{13} = \ldots = A_{nm}$ *– anisotropy coefficients of the plate material.*

The boundary conditions for the plate deformation problem due to transverse oscillations in this formulation can be represented in the form [16, 17]:

$$W = \frac{\partial^2 W}{\partial x^2} = 0; x = 0, l_1; \\ W = \frac{\partial W}{\partial y} = 0; y = 0, l_2. \qquad (9)$$

The solution of the homogeneous equation (7) is proposed to be sought in the following form:

$$W(x,y,t) = W(x,y)\exp\left(\xi \frac{bt}{h}\right), \qquad (10)$$

where ξ *– natural oscillation frequency of the plate.*

After substituting (10) into (7), we obtain:

$$A_1 W(x,y)\left(\frac{b\xi}{h}\right)^2 \exp\left(\xi\frac{bt}{h}\right) + \\ + A_2 W(x,y)\left(\frac{b\xi}{h}\right)^4 \exp\left(\xi\frac{bt}{h}\right) - \\ - A_3 \Delta W(x,y)\left(\frac{b\xi}{h}\right)^2 \exp\left(\xi\frac{bt}{h}\right) + \\ + A_4 \Delta^2 W(x,y)\exp\left(\xi\frac{bt}{h}\right) + \\ + A_5 W(x,y)\left(\frac{b\xi}{h}\right)\exp\left(\xi\frac{bt}{h}\right) + \\ + A_6 W(x,y)\left(\frac{b\xi}{h}\right)^3 \exp\left(\xi\frac{bt}{h}\right) + \\ + A_7 \Delta W(x,y)\left(\frac{b\xi}{h}\right)\exp\left(\xi\frac{bt}{h}\right) = 0. \qquad (11)$$

For the convenience of working with the mathematical model of a plate, it is expedient to use dimensionless quantities $x = \frac{l_1}{\pi}\alpha;\ y = \frac{l_2}{\pi}\beta$ *, by means of which the defining equation (11) can be represented in the following form:*

$$V(\alpha,\beta)\left(\begin{matrix} \left(\frac{\partial^4}{\partial\alpha^4} + 2\frac{l_1^2}{l_2^2}\frac{\partial^4}{\partial\alpha^2\partial\beta^2} + \frac{l_1^4}{l_2^4}\frac{\partial^4}{\partial\beta^4}\right) + \\ + B_1\left(\frac{l_1^2}{\pi^2}\frac{\partial^2}{\partial\alpha^2} + \frac{l_1^4}{\pi^2 l_2^2}\frac{\partial^2}{\partial\beta^2}\right) + \\ + B_2\frac{l_1^4}{\pi^4} \end{matrix}\right) = 0. \qquad (12)$$

Here we use the notation:

$$B_1 = \frac{1}{A_4}\left(\begin{matrix} -A_3\left(\frac{b\xi}{h}\right)^2 + \\ + A_7\left(\frac{b\xi}{h}\right) \end{matrix}\right);$$

$$B_2 = \frac{1}{A_4}\left(\begin{matrix} A_1\left(\frac{b\xi}{h}\right)^2 + A_2\left(\frac{b\xi}{h}\right)^4 + \\ + A_5\left(\frac{b\xi}{h}\right) + A_6\left(\frac{b\xi}{h}\right)^3 \end{matrix}\right).$$

To solve the equation (12) it is proposed to use the decomposition method [18], it allows us to consider separately three auxiliary problems, combining the results obtained.

1. $\frac{\partial^4 V_1}{\partial\alpha^4} = f_1(\alpha,\beta)\ V_1 = \frac{\partial V_1}{\partial\alpha} = 0\ \ \alpha = 0, \pi.$

2. $\eta^4 \frac{\partial^4 V_2}{\partial \beta^4} = f_2(\alpha,\beta)\ V_2 = \frac{\partial V_2}{\partial \beta} = 0\ \ \beta = 0, \pi.$ *(13)*

3. $$\begin{bmatrix} 2\eta^2 \frac{\partial^4}{\partial \alpha^2 \partial \beta^2} + \\ + B_1 \frac{l_1^2}{\pi^2}\left(\frac{\partial^2}{\partial \alpha^2} + \eta^2 \frac{\partial^2}{\partial \beta^2}\right) + \\ + B_2 \frac{l_1^4}{\pi^4} \end{bmatrix} V_3 + f_1 + f_2 = 0.$$

Here $\eta = l_1/l_2$, $f_i(\alpha,\beta) = \sum_{n,m=1}^{\infty} a_{n,m}^{(i)} \sin(n\alpha)\sin(m\beta)$ *– arbitrary functions in the general form;* $a_{n,m}^{(i)}$ *– arbitrary constants,* $i = 1,2$.

In determining the dynamic characteristics of the track behavior, taking into account the natural oscillations for its given points, it can be assumed that the following relations will be approximately satisfied:

$$V_1 \cong V_2;\ V_3 = \frac{1}{2}(V_1 + V_2). \quad (14)$$

The general solution of the auxiliary problems (13) is proposed to be sought within the variants:

$$\begin{aligned} V_1(\alpha,\beta) &= \sum_{n,m=1}^{\infty} \frac{a_{n,m}^{(1)}}{n^4} \sin(n\alpha)\sin(m\beta) + \\ &+ \frac{\alpha^3}{6}\psi_1(\beta) + \frac{\alpha^2}{2}\psi_2(\beta) + \alpha\psi_3(\beta) + \psi_4(\beta); \\ V_2(\alpha,\beta) &= \sum_{n,m=1}^{\infty} \frac{a_{n,m}^{(2)}}{\eta^4 m^4} \sin(n\alpha)\sin(m\beta) + \\ &+ \frac{\beta^3}{6}\phi_1(\alpha) + \frac{\beta^2}{2}\phi_2(\alpha) + \beta\phi_3(\alpha) + \phi_4(\alpha). \end{aligned} \quad (15)$$

where $\psi_i(\beta)$ *and* $\phi_i(\alpha)$ *– some arbitrary functions, for which it is necessary to take into account the boundary conditions (9) and defragmentation of the general problem (13).*

Determining $\psi_i(\beta)$ *and* $\phi_i(\alpha)$*, we get:*

for $\underline{\alpha = 0}$

$$V_1(\alpha,\beta) = \psi_4(\beta) = 0,\ \frac{\partial^2 V_1}{\partial \alpha^2} = \psi_2(\beta) = 0; \quad (16)$$

for $\underline{\alpha = \varpi}$

$$\psi_1(\beta) = 0, \psi_3(\beta) = 0,$$

$$V_1(\alpha,\beta) = \sum_{n,m=1}^{\infty} \frac{a_{n,m}^{(1)}}{n^4} \sin(n\alpha)\sin(m\beta); \quad (17)$$

for $\underline{\beta = 0}$

$$V_2(\alpha,\beta) = \phi_4(\alpha) = 0,\ \phi_3(\alpha) = -\sum_{n,m=1}^{\infty} \frac{a_{n,m}^{(2)}}{\eta^4 m^3} \sin(n\alpha); \quad (18)$$

for $\underline{\beta = \varpi}$

$$\phi_1(\alpha) = -\frac{6}{\pi^2} \sum_{n,m=1}^{\infty} \frac{a_{n,m}^{(2)}}{\eta^4 m^3} \sin(n\alpha)\left((-1)^m + 1\right),$$

$$\phi_2(\alpha) = \frac{2}{\pi} \sum_{n,m=1}^{\infty} \frac{a_{n,m}^{(2)}}{\eta^4 m^3} \sin(n\alpha)\left((-1)^m + 2\right). \quad (19)$$

$$V_2(\alpha,\beta) = \sum_{n,m=1}^{\infty} \frac{a_{n,m}^{(2)}}{\eta^4 m^3} \sin(n\alpha) \begin{pmatrix} \frac{1}{m}\sin(m\beta) - \\ -\frac{\beta^3}{\pi^2}\left((-1)^m + 1\right) + \\ + \frac{\beta^2}{\pi}\left((-1)^m + 2\right) - \beta \end{pmatrix}.$$

As a result, from (13) we have the following system of equations:

$$\begin{cases} V_1 - V_2 = 0,\ V_3 = \frac{1}{2}(V_2 + V_1), \\ \begin{bmatrix} 2\eta^2 \frac{\partial^4}{\partial \alpha^2 \partial \beta^2} + \\ + B_1 \frac{l_1^2}{\pi^2}\left(\frac{\partial^2}{\partial \alpha^2} + \eta^2 \frac{\partial^2}{\partial \beta^2}\right) + \\ + B_2 \frac{l_1^4}{\pi^4} \end{bmatrix} V_3 + f_1 + f_2 = 0. \end{cases} \quad (20)$$

For $n,m = 1$ *from (20) we fix the ratios:*

$$\begin{cases} a_{11}^{(1)} \sin(\alpha)\sin(\beta) - \frac{a_{11}^{(2)}}{\eta^4}\sin(\alpha)\left(\sin(\beta) + \frac{\beta^2}{\pi} - \beta\right) = 0, \\ \left[2\eta^2 \frac{\partial^4}{\partial \alpha^2 \partial \beta^2} + B_1 \frac{l_1^2}{\pi^2}\left(\frac{\partial^2}{\partial \alpha^2} + \eta^2 \frac{\partial^2}{\partial \beta^2}\right) + B_2 \frac{l_1^4}{\pi^4}\right]\frac{1}{2} \bullet \\ \bullet\left(a_{11}^{(1)} \sin(\alpha)\sin(\beta) + \frac{a_{11}^{(2)}}{\eta^4}\sin(\alpha)\left(\sin(\beta) + \frac{\beta^2}{\pi} - \beta\right)\right) + \\ + a_{11}^{(1)} \sin(\alpha)\sin(\beta) + a_{11}^{(2)} \sin(\alpha)\sin(\beta) = 0. \end{cases}$$

Assuming $\alpha = \beta = \frac{\pi}{2}$ *in the previous relations, we obtain a system of equations that has a nonzero solution only if its principal determinant is equal to zero:*

$$\begin{aligned} &B_1 \frac{l_1^2}{\pi^2 \eta^2}\left[\left(\frac{1}{\eta^2} + \frac{1}{2}\right)\left(1 - \frac{\pi}{4}\right) - \left(\frac{2}{\pi} - 1\right)\right] - \\ &- B_2 \frac{l_1^4}{\pi^4 \eta^4}\left(1 - \frac{\pi}{4}\right) - \frac{1}{\eta^4}\left(2 - \frac{\pi}{4} - \frac{2}{\pi}\right) - 1 = 0. \end{aligned} \quad (21)$$

If we substitute expressions for B_1 *and* B_2 *in (21), we obtain:*

$$\begin{aligned} &\frac{1}{A_4}\left(-A_3\left(\frac{\xi b}{h}\right)^2 + A_7\left(\frac{\xi b}{h}\right)\right)\frac{l_1^2}{\pi^2 \eta^2} \bullet \\ &\bullet\left[\left(\frac{1}{\eta^2} + \frac{1}{2}\right)\left(1 - \frac{\pi}{4}\right) - \left(\frac{2}{\pi} - 1\right)\right] - \\ &- \frac{1}{A_4}\begin{pmatrix} A_2\left(\frac{\xi b}{h}\right)^4 + A_6\left(\frac{\xi b}{h}\right)^3 + \\ + A_1\left(\frac{\xi b}{h}\right)^2 + A_5\left(\frac{\xi b}{h}\right) \end{pmatrix}\frac{l_1^4}{\pi^4 \eta^4}\left(1 - \frac{\pi}{4}\right) - \\ &- \frac{1}{\eta^4}\left(2 - \frac{\pi}{4} - \frac{2}{\pi}\right) - 1 = 0. \end{aligned} \quad (22)$$

Equation (22) can be represented in the form of an algebraic equation of the fourth order, the unknown in which is the frequency of natural oscillations of the ballastless track

$$d_1\xi^4 + d_2\xi^3 + d_3\xi^2 + d_4\xi + d_5 = 0. \quad (23)$$

Here we have adopted the following notation for the coefficients of unknowns:

$$d_1 = -\frac{A_2}{A_4}\frac{l_1^4}{\pi^4\eta^4}\left(1-\frac{\pi}{4}\right)\left(\frac{b}{h}\right)^4,$$

$$d_2 = -\frac{A_6}{A_4}\frac{l_1^4}{\pi^4\eta^4}\left(1-\frac{\pi}{4}\right)\left(\frac{b}{h}\right)^3,$$

$$d_3 = \frac{l_1^2}{A_4\pi^2\eta^2}\left\{\begin{array}{l} A_3\left[\left(\frac{1}{\eta^2}+\frac{1}{2}\right)\left(1-\frac{\pi}{4}\right)+\frac{1}{2}-\frac{1}{\pi}\right]- \\ -A_1\frac{l_1^2}{\pi^2\eta^2}\left(1-\frac{\pi}{4}\right) \end{array}\right\}\left(\frac{b}{h}\right)^2,$$

$$d_4 = \frac{l_1^2}{A_4\pi^2\eta^2}\left\{\begin{array}{l} \frac{A_7}{2}\left[\frac{1}{2}-\frac{1}{\pi}+\frac{3}{2}\left(1-\frac{\pi}{4}\right)\right]- \\ -A_5\frac{l_1^2}{\pi^2\eta^2}\left(1-\frac{\pi}{4}\right) \end{array}\right\}\left(\frac{b}{h}\right),$$

$$d_5 = \frac{1}{\eta^2}\left[\left(-1+\frac{\pi}{4}\right)\left(1+\frac{1}{\eta^2}\right)-1+\frac{2}{\pi}\right]-1.$$

Solving the equation (23), we can determine the frequencies of natural oscillations of the railway track, which in turn will allow us to determine the dynamic normal displacement of points of the track upper structure [19, 20] and of the plate of the ballastless base according to the formula (10).

3.

The traditional ways of calculating the parameters of the behavior of the railway track both because of the movement of vehicles and due to natural oscillations do not allow to fully take into account the anisotropic properties of the track design, especially a ballastless one, in straight and curved sections [7, 15, 21].

We have studied the data obtained and built the graph dependences of dynamic deflections, which is modeled by a transversally isotropic plate, on time for different ratios of elastic moduli and shear moduli [13, 22]. The parameters of the dynamic impact of the vehicle on the track take the following values: m = 25 t, h = 500 mm, V_0 = 20 m/s, $\rho = 7850$ kg/m^3.

Using relations (10) for the dynamic deflection recorded in a dimensionless form, we obtain graphs of the dependences of the dynamic characteristics on time [12, 23].

Pic. 3 shows the dependence of the dynamic deflection of the track upper structure on time for different values of the ratio E_θ/E_r (the ratio of the reduced elastic moduli in the direction of the sleeper and the rail, respectively), which are indicated as the numbers in the curves. The influence of the anisotropic properties of the plate of the ballastless base on the characteristics of the dynamic effect is considered: with decreasing ratio E_θ/E_r, the deflection-sediment increases to a certain value at E_θ/E_r <1; with increasing E_θ/E_r, the deflection decreases, since the last term of the segment of the series obtained from (10) decreases with increasing ratio E_θ/E_r > 1.

Pic. 4 shows depressions of the ballastless track, assuming that it has transversely isotropic properties for various shear moduli in the direction perpendicular to the plane of the embankment (G_{rz}), for different ratios of the shear modulus in the direction perpendicular to the rails, and the strain modulus in the direction of the thread. The values G_{rz}/E_r are shown in digits at the curves, at G_{rz}/E_r = 0,54 the ballast prism has isotropic properties. From Pic. 4 it follows that the increase in the value of the modulus ratio G_{rz}/E_r leads to a decrease in deflection-sediment.

The dashed line in Pic. 3 and Pic. 4 shows the depressions determined experimentally on the approach to the bridge over the Goryuchka River (even track), the bridge located on the section Saratov–Kolotsky at 56 km. By comparison with the curves obtained theoretically based on the proposed model, it is possible to estimate the resulted rigidity (modulus of elasticity and shear) of the track under consideration at the approach to the bridge. As a result, there is a good consistency between the results of the experiment and the analytical calculation of the largest deflection value and the duration of the deformation at the track, only at the beginning the experimental dependence behaves more linearly than the theoretical dependence.

Pic. 5 shows the dependence of the maximum deflection on the ratio E_θ/E_r for different values of the reduced strain modulus of the track upper structure $\tilde{E}$: curve 1 corresponds to $\tilde{E}$ = 3,6 • 10^{-6}, curve 2 – $\tilde{E}$ = 2,5 • 10^{-6}, curve 3 – $\tilde{E}$ = 1,4 • 10^{-6}. From Pic. 5 it follows that the maximum deflection decreases with increasing ratio E_θ/E_r and increases with increasing linear rigidity of the wheel–rail contact $\tilde{E}$. It is equally clear that as the ratio E_θ/E_r increases, the dynamic deflection decreases for all considered wheel–rail contact rigidity ratios.

Simultaneously, the movements of the base of the plate of the ballastless track in the zone of its contact with the ground of the embankment were determined.

In Pic. 6a it is shown that when the moduli of elasticity E_r and E_θ decrease and the maximum value of the dynamic deflection increases, and E_r has the greatest effect on deflection. When the values of shear moduli decrease, the deflection increases, while the graph of Pic. 6b shows that $G_{\theta z}$ affects the dynamic deflection of the target more than other parameters.

When decreasing $G_{rz}, G_{\theta z}$, the greatest deflection and time during which the deflection is equated to zero increase proportionately, and when decreasing $G_{r\theta}$, the time related to the zero deflection increases more intensively; i. e. restoration of the roadbed will be slower.

Comparing the graphical dependencies for the dynamic depression, it is possible to select the mechanical characteristics of the embankment with anisotropic properties (search for different structures for the transitional sections of variable rigidity) in such a way as to reduce the depression to the level necessary for train movement at a given speed, and the maximum force at which there will be no defects in the roadbed.

Conclusions. *Analyzing and comparing the theoretical dependences obtained for different values of the mechanical parameters of the roadbed with the calculated data, it is easy to find that by changing the mechanical parameters of the soil, it is possible both to increase and reduce the deformation of the railway track. High compliance of the data of mathematical modeling with the results* *of experimental research makes it possible to recommend the proposed method as a tool of solving problems that ensure the stability of the behavior of the railway track when operating existing lines and when designing high-speed lines.*

REFERENCES

1. Instruction on the use of structural and technological solutions of transition areas at approaches to artificial structures for high-speed combined traffic areas. Approved by the order of JSC Russian Railways of December 20, 2013, No. 2754r [*Instruktsiya po primeneniyu konstruktivno-tehnologicheskih reshenii perehodnyh uchastkov na podhodah k iskustvennym sooruzheniyam dlya uchastkov skorostnogo sovmeshchennogo dvizheniya. Utverzhdena rasporyazheniem OAO «RZD» ot 20.12.2013 No. 2754r*].

2. Coelho, B., Priest, J., Hölscher, P., Powrie, W. Monitoring of transition zones in railways, 10th International Conference and Exhibition on railway engineering, London, 24–25 June, 2009.

3. Konshin, G. G. Operation of the road bed under the trains [*Rabota zemlyanogo polotna pod poezdami*]. Moscow, TMC for education on railway transport, 2012, 208 p.

4. Loktev, A. A., Vinogradov, V. V., Buchkin, V. A. Models of interaction of wheel and rail at high speed. *World of Transport and Transportation*, Vol. 14, 2016, Iss. 1, pp. 54–60.

5. Loktev, A., Sychev, V., Gridasova, E., Stepanov R. Mathematical Modeling of Railway Track Structure under Changing Rigidity Parameters. Nonlinearity. Problems, Solutions and Applications. Vol. 1. Theoretical and Applied Mathematics, 2017, pp. 291–307

6. Kiselev, F. B., Mansurov, A. R., Ramazanov, M. I. Modeling of the dynamic effect of a rolling stock on the base of a railway embankment with a cylindrical cavity [*Modelirovanie dinamicheskogo vozdeistviya podvizhnogo sostava na osnovanie zheleznodorozhnoi nasypi s tsilindricheskoi polost'yu*]. *Vnedrenie sovremennyh konstruktsii i peredovyh tehnologii v putevoe hozyaistvo*, 2016, Iss. 10, pp. 37–45.

7. Abdurashitov, A. Yu., Sychev, V. P., Abdurashitov, Yu. A. Choice of models of the stressed-deformed state of railway rails under different variants of their hardening [*Vybor modelei napryazhenno-deformirovannogo sostoyaniya zheleznodorozhnyh rel'sov pri razlichnyh variantah ih zakalivaniya*]. *Vnedrenie sovremennyh konstruktsii i peredovyh tehnologii v putevoe hozyaistvo*, 2016, Iss. 10, pp. 64–79.

8. Loktev, A. A. Shock interaction of a solid body and an elastic orthotropic plate [*Udarnoe vzaimodeistvie tverdogo tela i uprugoi ortotropnoi plastinki*]. *Mehanika kompozitsionnyh materialov i konstruktsii*, 2005, Iss. 4, pp. 478–492.

9. Loktev, A. A., Sychev, V. P. Vinogradov, V. V., Buchkin, V. A. Modelling of the Dynamic Contact between a Wheel of a Moving Railway Vehicle and Rails with Evaluation of Defects Emerging upon Their Interaction. Part 1. The Defects of the Rail and Models of Contact. *Applied Mathematical Sciences*, 2017, Vol. 11, No. 10, pp. 473–480.

10. Sychev, V. P., Novozhilov, T. V. Research of influence of damping pads under rails and sleepers on the railway track [*Issledovanie vliyaniya na rabotu zheleznodorozhnogo puti dempfiruyushchih podkladok pod rel'sy i shpaly*]. *Nauka i tehnika transporta*, 2016, Iss. 1, pp. 63–68.

11. Zaletdinov, A. V., Loktev, A. A., Sycheva, A. V., Zapolnova, E. V. Selection of sites for reinforcement of the roadbed [*Vybor mest usileniya zemlyanogo polotna*]. *Put' i putevoe hozyaistvo*, 2015, Iss. 3, pp. 15–18.

12. Agostinacchio, M., Ciampa, D., Diomedi, M., Olita, S. Parametrical analysis of the railways dynamic response at high speed moving loads. *Journal of Modern Transportation*, 2013, Vol. 21, No. 3, pp. 169–181.

13. Phillips, J. W., Calvit, H. H. Impact of a rigid sphere on a viscoelastic plate. Transaction of the ASME, *Journal of Applied Mechanics*, 1967, Vol. 34, No. 4, pp. 873–878.

14. Starishkin, V. V., Fazilova, Z. T. Sites of transitional rigidity in the zone of conjunction to bridges with ballast and ballastless track design [*Uchastki perehodnoi zhestkosti v zone primykaniya k mostam s ballastnoi i bezballastnoi konstruktsiei puti*]. *Vnedrenie sovremennyh konstruktsii i peredovyh tehnologii v putevoe hozyaistvo*, 2017, Iss. 11, pp. 16–20.

15. Chen, P., Xiong, J., Shen, Z. Thickness effect on the contact behavior of a composite laminate indented by a rigid sphere. *Mechanics of Materials*, 2008, Vol. 40, pp. 183–194.

16. Sycheva, A. V., Sychev, V. P., Buchkin, V. A., Bykov, Yu. A. Modeling the work of a railway track as a system of quasielastic orthotropic layers [*Modelirovanie raboty zheleznodorozhnogo puti kak sistemy kvaziuprugih ortotropnyh sloev*]. *Vestnik MGSU*, 2016, Iss. 3, pp. 37–46.

17. Malekzadeh K., Khalili M. R., Mittal R. K. Response of composite sandwich panels with transversely flexible core to low-velocity transverse impact: A new dynamic model. *Int. J. of Impact Engineering*, 2007, Vol. 34, pp. 522–543.

18. Loktev, A. A., Impact of a viscoelastic body on an elastic isotropic plate [*Udar vyazkouprugogo tela po uprugoi izotropnoi plastinke*]. *Mehanika kompozitsionnyh materialov i konstruktsii*, 2007, Iss. 3, pp. 417–425.

19. Vershinin, V. V., Loktev, A. A. Modeling of systems of shockproof insulation with viscoelastic elements [*Modelirovanie system protivoudarnoi izolyatsii s vyazkouprugimi elementami*]. *Vestnik of Bauman MSTU. Series of Natural Sciences*, 2012, Iss. 2, pp. 52–67.

20. Loktev, A. A. Elastic-plastic model of the interaction of a cylindrical impactor and a plate [*Uprugoplasticheskaya model' vzaimodeistviya tsilindricheskogo udarnika i plastinki*]. *Pis'ma v journal tehnicheskoi fiziki*, 2007, Iss. 16, pp. 72–77.

21. Loktev, A. A., Bakhtin, V. F., Chernikov, I. Yu., Loktev, D. A. Methodology for determining external defects of a structure by analyzing a series of its images in a monitoring system [*Metodika opredeleniya vneshnih defektov sooruzheniya putem analiza sesrii ego izobrazhenii v sisteme monitoring*]. *Vestnik MGSU*, 2015, Iss. 3, pp. 7–16.

22. Alfimtsev, A. N., Loktev, D. A., Loktev, A. A. Comparison of methodologies for development of intellectual interaction systems [*Sravnenie metodologii razrabotki system intellektual'nogo vzaimodeistviya*]. *Vestnik MGSU*, 2013, Iss. 5, pp. 200–208.

23. Loktev, A. A., Sycheva, A. V., Talashkin, G. N., Stepanov, K. D. Development of the mathematical model of a railway track of variable rigidity [*Razrabotka matematicheskoi modeli zheleznodorozhnogo puti peremennoi zhestkosti*]. *Vnedrenie sovremennyh konstruktsii i peredovyh tehnologii v putevoe hozyaistvo,* 2016, Iss. 9, pp. 26–38. ●

Information about the authors:

Vinogradov, Valentin V. – D.Sc. (Eng), professor of Russian University of Transport, Moscow, Russia, +7(495) 684–21–10.

Loktev, Alexey A. – D.Sc. (Physics and Mathematics), professor, head of the department of Transport construction of Russian University of Transport, Moscow, Russia, aaloktev@yandex.ru.

Fazilova, Zulfiya T. – Ph.D. (Eng), associate professor of Russian University of Transport, Moscow, Russia, fazil_1905@mail.ru.

Article received 22.03.2018, accepted 19.05.2018.